XVIII IMEKO WORLD CONGRESS
Metrology for a Sustainable Development
September, 17 – 22, 2006, Rio de Janeiro, Brazil

ON-LINE WEAR DETECTION OF MILLING TOOLS USING A DISPLACEMENT FIBER OPTIC SENSOR

Guillermo de Anda-Rodríguez [1], *Eduardo Castillo-Castañeda* [2], *Salvador Guel-Sandoval* [3], *Juan Hurtado-Ramos*[4], *Maria Eugenia Navarrete-Sánchez* [5]

[1] Instituto Tecnológico de San Luis Potosí. Departamento de Metalmecánica. Av. Tecnológico s/n, San Luis Potosí, S.L.P. 78437, México, memodeanda@yahoo.com.mx
[2] Universidad Autónoma de Querétaro. Facultad de Ingeniería, Cerro de las Campanas s/n, Querétaro 76010, México, ecast@uaq.mx
[3]Instituto de Investigación en Comunicación Óptica, UASLP, S.L.P., México, sguel@cactus.iico.uaslp.mx
[4]Instituto Politécnico Nacional, CICATA, Querétaro, México, jhurtadoramos@cicataqro.ipn.mx
[5] Instituto Tecnológico de San Luis Potosí. Departamento de Sistemas y Computación . SLP, México, marun99@yahoo.com

Abstract: One of the major problems in precision machining processing can be related to the failure condition of the cutting tool. Hence online tool condition-monitoring is of much interest in metal-mechanics industry. The spontaneous problem of failure in a cutting tool, such as chipping and breakage, is becoming more and more important in the manufacturing technology and is usually associated with the stresses put on the tool during the cutting process. Other abnormal tool conditions in metal-machining includes: tool wear, tool-work piece, etc.
In this work a method is presented for determining the wear and fracture of a cutting tool, by means of a fiber optic sensor with high resolution and large bandwidth, used during the manufacturing process. The sensor has been configured with two groups of fibers, distributed in a random fashion. One of the groups works as a light emitter that illuminates the tool, while the other captures the light reflected by the tool surface itself. The light is generated by a photodiode, which does not represent any risk to the health. This technique will allow observing the wear and breakage of the tool in real time while the tool is rotating, with a high degree of accuracy.

Keywords: Fiber optic sensor, tool wear , tool breakage.

1. INTRODUCTION

The need for high level of automation, of manufacturing operations. Successful implementation of this demands uninterrupted machining for longer duration with least human supervision. In such situations, unfavorable conditions like tool wear, tool breakage, chip-form and work piece roughness must be monitored on-line, to reduce possibilities of interruptions during machining. Of these, monitoring of tool wear Is critical due to its substantial influence on the required surface finish and desired dimensional accuracy.
Various techniques have been proposed for recognition of tool status based on monitoring of cutting forces, temperature, vibration, power and Acoustic Emission [10]. Each technique has its own advantages and limitations; however, no single technique has proved to be completely reliable over a range of operating conditions**.** This has prompted the need for a system that integrates information from different monitoring sensors.

This paper describes the possibility of sensor in a machining process through a technique for on-line wear monitoring of a milling tool. The tool wear is estimated directly from a fiber optic sensor with high resolution and high bandwidth characteristics. This sensor provides a distance measurement between its probe and the tool profile. The contribution of this work is the application of this sensor to sense on-line wear of a milling tool. Since the light emitted by this sensor comes from a photodiode, it does not produce eye damage; this is safer than laser displacement sensors. This technique senses the tool wear in real time, while the tool is rotating, with accuracy less than 1 micron. Experimental results are also presented for a four-flank cutting tool rotating at 300 rpm.
Tool Condition Monitoring (TCM) is concerned with assessing the condition of the tool during machining, by measuring factors that influenced by tool status (chipping, wear and breakage), and comparing with pre-set criteria for deciding action. Traditionally TCM has been undertaken by machine operators. A human operator can asses the status of the tool by observing the associated changes (chip form, color, sound due to rubbing, damage of surface finish etc.) during machining operation. However continuous assessment of tool status is gaining importance for avoiding undesirable machining and frequent interruptions. Further, in manufacturing situations such as, unmanned, least attended and longer operations, monitoring system is expected to substitute the knowledge, experience, sensory and pattern recognition abilities of the human operator**.** Figure 1 This can be achieved by adopting a decision making scheme which can interpret information from sensors, learn from the environment, adjust itself in response

to knowledge gained during the learning process and decide on the appropriate action. This calls for an Intelligent Tool Condition monitoring (ITCM) system. Such system includes various sensors, signal conditioning devices, signal processing algorithms and signal interpretation and decision making**.** As stated earlier, various tool wear sensing methods have been proposed and evaluated. However, none of these methods were universally successful due to the complex nature of the machining processes **.** In general, these could be broadly classified into direct and indirect methods [9] as shown in Table I. Of course, in normal practice, indirect methods are more popular owing to the fact that these are easy to handle and relatively economical.

Table 1 Tool wear sensing techniques

Direct	**Indirect**
Electrical Resistance	Torque and Power
Optical	Temperature
Contact Sensing	Vibration
Radioactive	Cutting Forces
	Acoustic Emission

1.1 The cutting process

The cutting process presents a particular problem. There are several input variables to the process such as:
Cutting, speed, Feed rate, Depth of the cut, Tool and work piece material properties, etc. These parameters at the beginning of any experience are fixed and define the It operation conditions figure 2. From here, the experimental results will be valid just for a particular case. All the changes of the operation conditions are reflected in the output variables. Some of these variables are: Cutting temperature, Chip thickness, Cutting forces, Surface finish, tool wear**,** etc. Most of these parameters can be measured to a certain degree. However, measuring the wear of the cutting tool on-line is very difficult but, it is possible to estimate it by detecting a process parameter correlated with tool wear. The wear of the cutting tool is often the most accepted criterion for tool life**.** Cutting tool life does not represent the physical life of the tool, but the economic life of the tool in the real sense. There are three important wear zones: Flank wear, crater wear and nose radius wear. Flank wear is considered the most important criterion for tool life.
Significant research has been done on cutting force-based tool flute breakage detection [2,3,4,5]. The technique is dependent upon the instantaneous load applied to the cutter and has the advantage of being easily modeled. Cutting force measurements are commonly taken using a dynamometer mounted on a machining worktable, or a mounted tool holder during machining. The dynamometer is an essential tool for experimental work, and has been proved a very successful tool in establishing inter-relationships between secondary machining parameters and cutting force, so as to enable researchers to prove their tool monitoring strategies prior to implementing them on-line. However, the physical characteristics of the dynamometer mounted on the worktable seriously limit the physical size of the work piece, on the other hand, mounted in on the tool holder interrupts the change of cutting tools, and the cost of the dynamometer is very high. Additionally, the cutting force-based methods often require complex signal processing techniques, like high-order time series models, and FFT, as well as time frequency analysis, which result in a hindrance to real time application due to the computation time. Acoustic emission (AE), is a very high frequency stress wave, generated when deformation occurs when metals are cut or fractured, which is linked to the plastic deformation process occurring during chip formation due to the interaction between the work piece and cutting tool [2,3]

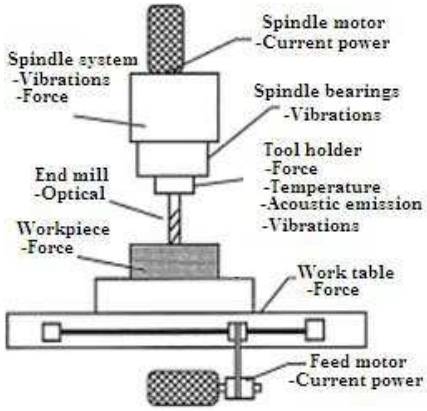

Fig. 1. Approaches of tool breakage monitoring for end milling operations.

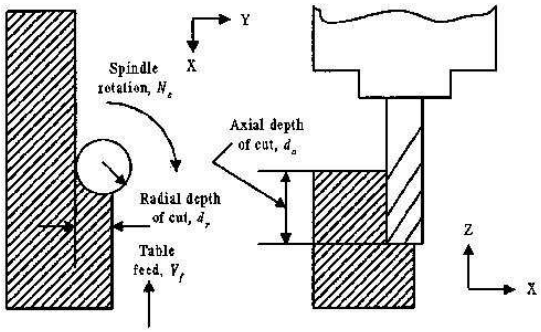

Fig. 2 The milling cutting process

2. THE DISPLACEMENT FOTONIC SENSOR

2.1 The fiber sensor

The recent growth of activity in fiber optic sensors has lead to a great variety of technically sophisticated devices employing interference, polarization, and wavelength modulation techniques [12]. In spite of all, these methods offer great promise to certain specific applications and dedicated sensors, the intensity modulated Fiber Optic Displacement Sensor offers a powerful combination of simplicity, performance, versatility, and low cost, which make it well suited for a wide variety of laboratory and industrial applications. Moreover, since the light emitted by this type of sensor comes from a photodiode it does not produce eye damage, then it is safer than laser displacement sensors.

2.2 Parameter analysis

The basic principle employed in the Fiber Optic Lever Displacement Transducer [13] is to use two sets of fiber optic elements, one to carry light from a remote source to an object or target whose displacement or motion is to be measured, and the other to receive the light reflected from the object and carry it back to a photo sensitive detector. A very common fiber optic probe is a bifurcated bundle fiber [14], as shown in Figure 3.

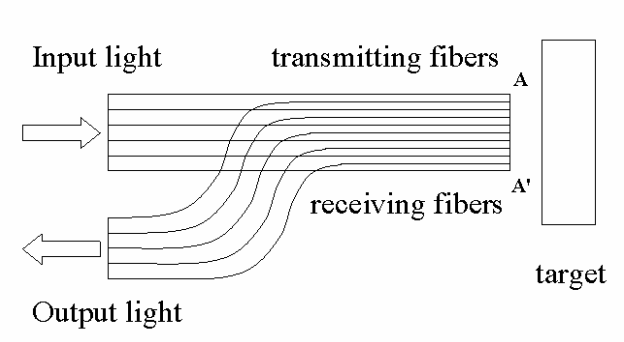

Fig. 3 Bifurcated bundle fiber

The light emitted from one bundle is back-reflected by the target and collected by another bundle (receiving fibers). As a result, the returned light at the detector is distance-modulated. The mathematical analysis of a photonic sensor is considerably simplified by the assumption that uni-angular electro luminescent energy is coupled into loss-less, non-dispersing, and otherwise ideal step-index fibers with negligible cladding thickness. Further simplification results when the sensor consists of a single centered transmitting fiber surrounded by six symmetrical receiving fibers (radius equal to r_0) as shown in Figure 4. This figure shows the exit and reflected patterns at the exit/return plane. The area of receiving fibers illuminated by reflected light (reflected ring radius x) is proportional to the target distance y (standoff distance). The distance dx represents x variations when distance from probe to target varies (dy). The characteristic parameters associated to this sensor can be determined from the knowledge of: the angle ϕ and the emittance level of the exit illumination, the geometric relationships between transmitting and receiving fibers, and the distance from fiber-tip to target.

The mathematical relationships of the displacement sensor, such as: the geometric sensitivity, the displacement sensitivity, the optical detection limit, and the displacement detection limit, will be derived in the next section. In this work, the *sensitivity* was defined as the rate of change of the standoff distance due to a change in a parameter.

The geometric sensitivity (α_G) is defined as the relationship between the standoff distance variations and the distance-modulated area of reflected light on the fiber termination plane, i.e., $\alpha_G = \dfrac{dy}{dA}$

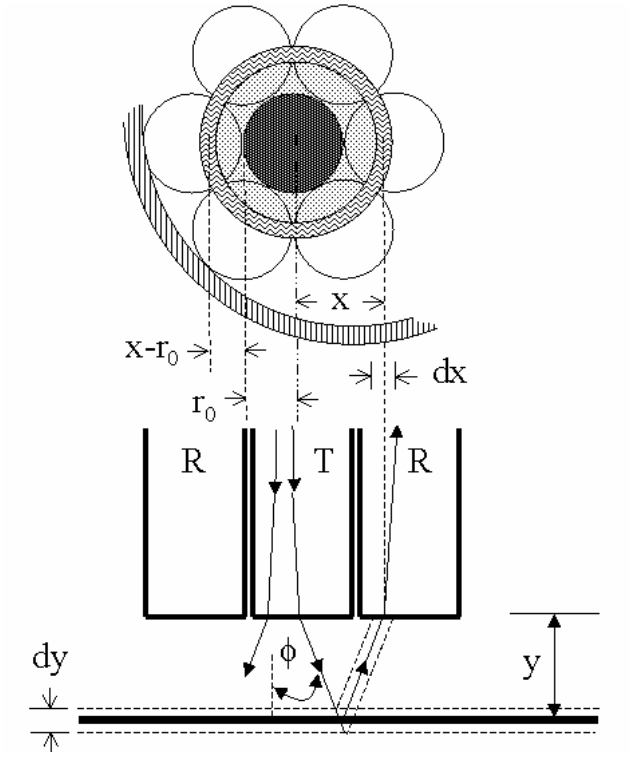

Fig. 4. Cross section of the sensor

From trigonometry, it is a function of the fiber radius and illumination exit angle only. When fiber cladding is negligible, the standoff distance is given by

$$y = \frac{x - r_0}{2\tan\phi} \tag{1}$$

By defining a parameter $q = x / r_0$, the equation (1) can be rewritten as

$$y = \frac{(q-1)r_0}{2\tan\phi} \tag{2}$$

The distance-modulated area of the reflected ring on the fiber termination plane is given by $dA = 2\pi\, x dx$.

The first derivative of equation (2) respect to this area is given by:

$$\frac{dy}{dA} = \frac{1}{2\tan\phi}\frac{dx}{dA} \tag{3}$$

Then the α_G referred to this plane is

$$\frac{dy}{dA} = \frac{1}{4\pi\, x\tan\phi} \tag{4}$$

The displacement sensitivity (α_D) of a fiber optic sensor is determined by the manner in which the optical radiometric

power (p_{OR}) reaching the photo-detector varies with the target distance, i.e., $\alpha_D = \dfrac{dy}{dp_{OR}}$

The nonlinear contributions of the α_D are incorporated into a term $\tilde{s} = dq / d\tilde{p}_{OR}$, where $\tilde{p}_{OR} = \dfrac{p_{OR}}{p_{\max}}$. $p_{\max}$ is the maximum subtended power. The differentiation of this term and equation (4) lead to:

$$\alpha_D = \frac{\tilde{s} r_0}{2 p_{\max} \tan\phi} \tag{5}$$

The subtended power of the receiving fibers is the product of the receiving fiber subtended area and the irradiance. Figure 5 shows the interaction of three adjacent transmitting and receiving fibers as the light is reflected from a target a the single angle ϕ. It can be seen that a zero gap, the light in the transmitting fiber would be reflected directly back into itself and little or no light would be transferred to the receiving fiber. As the gap increases, some of the reflected light is captured by the receiving fiber and carried to the photo sensitive detector. As the gap increases, a distance will be reached at which a maximum of reflected light is transferred to the receiving fiber. Further increases in the gap will result in a decrease in the light at the receiving fiber face and a corresponding drop in the output signal from the photo sensor. The gap and displacement range over which the initial rise in signal takes place and at which the maximum occurs is primarily determined by the diameter and the numerical aperture of the fibers and the intensity distribution within the operating filed of the fibers. In order to obtain the higher levels of intensity at the photo detectors, commercial devices of this type uses multiple transmitting and receiving fibers. The irradiance of the target-reflected illumination on the entrance plane of the receiving fibers may be derived from the geometry shown in Figure 5. Indeed, since all rays are meridional and uniformly distributed within the illuminated fiber, they exit at the single angle ϕ. Figure 5 shows that two different irradiances appear on a target located on plane B, a uniformly bright spot surrounded by a uniformly annular ring portion. When the target distance reaches the C plane the bright spot disappears and an annular ring appears (from C plane to target plane). The width of this annular ring is equal to the fiber diameter.

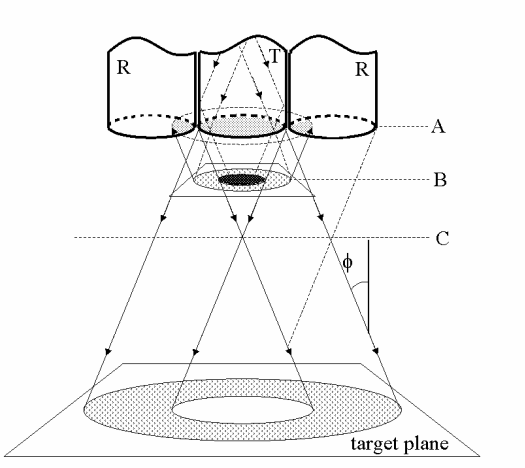

Fig. 5. Interaction between transmitting and receiving fibers

These two irradiances appear from zero to plane C. Figure 6 shows more clearly that patterns of reflected light on B and C planes are annular rings, diverging cone, and not uniformly illuminated disks since the rays exit the illuminating fiber are not perpendicular to those planes.

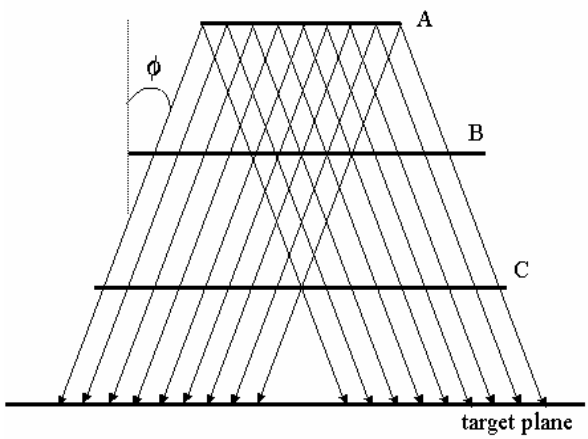

Fig. 6. Reflected patterns

The C plane distance is given by

$$\overline{AC} = \frac{r_0}{\tan\phi} \tag{6}$$

The optical detection limit (β_{OD}) is determined by the ability of the photo-detector to solve even smaller modulations in radiometric power. It can be determined from the shot-noise relationship [15]

$$I_{SH} = \left(p_{OR}\gamma 2eBW\right)^{1/2} \tag{7}$$

then the β_{OD} is given by

$$\beta_{OD} = \frac{I_{SH}}{\gamma} \tag{8}$$

where I_{SH} is the RMS noise current, γ is the responsitivity of the photo-detector, e is the electron charge, and BW is the noise current bandwidth.

The displacement detection limit (β_{DD}) of fiber sensors is the product of the α_D in displacement per watt and the optical detection limit (β_{OD}) in watts, i.e.,

$$\beta_{DD} = \alpha_D \beta_{OD} = \tilde{s}\left[\frac{r_0}{2\, p_{\max} \tan\phi}\right]\frac{(p_{OR}\gamma 2eBW)^{1/2}}{\gamma} \qquad (9)$$

Defining $\tilde{d} = \tilde{s}(\tilde{p}_{OR})^{1/2}$, equation (9) becomes

$$\beta_{DD} = \tilde{d}\,\frac{p_{\max}^{1/2}}{p_{OR}^{1/2}}\left[\frac{r_0}{2\, p_{\max} \tan\phi}\right]\frac{(p_{OR}\gamma 2eBW)^{1/2}}{\gamma} \qquad (10)$$

that can be reduced to

$$\beta_{DD} = \tilde{d}\,\frac{r_0}{\tan\phi}\left(\frac{eBW}{2p_{\max}\gamma}\right)^{1/2} \qquad (11)$$

Since nothing in the fiber optic sensors limits the bandwidth, this is determined only by the electronic circuitry. Some of the numerical values of the previous parameters are presented in the next section and were verified experimentally. The work presented in [16] gives additional information on the theoretical and experimental verification of the parameters of multiple fiber transducers.

2.3 The Sensor Probe

The photonic sensor that has been used in this work, shown in Figure 7, is a fiber-optic device model KD-300 from MTI Instruments, provided with a sensor probe MTI-2125-R.

Fig. 7. The displacement fiber optic sensor

This fiber-optic probe has two groups of optical fibers bundled together in a random configuration, as shown in Figure 8. The sensor converts the amount of reflected light into an electrical signal that is proportional to the distance from the probe to the target surface. The response curve that correlates the voltage output of the sensor and the gap to the target surface is shown in Figure 11. The initial rising portion of the curve, the front slope, is very sensitive and is the operating range used for high accuracy measurements. The declining section of the curve, the back slope, is used for measurements that require greater standoff distances.

In the analysis of sensitivity of the sensor presented in this work, the reflected light was assumed a good reflection in order to simplify the drawings, however the reflection light on the surface of the milling tool is evidently diffuse reflection.

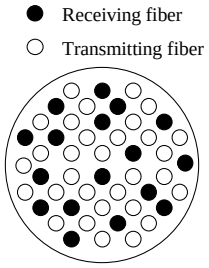

Fig. 8. Fiber distribution

In the analysis of sensitivity of the sensor presented in this work, the reflected light was assumed a good reflection in order to simplify the drawings, however the reflection light on the surface of the milling tool is evidently diffuse reflection.

3. THE EXPERIMENTAL SETUP

The experimental setup for this work is composed by a DENFORD VMC 3-axis milling machine, a data acquisition board with sample period of 150 KHz, the displacement photonic sensor, and a PC with a Pentium processor at 400 MHz.

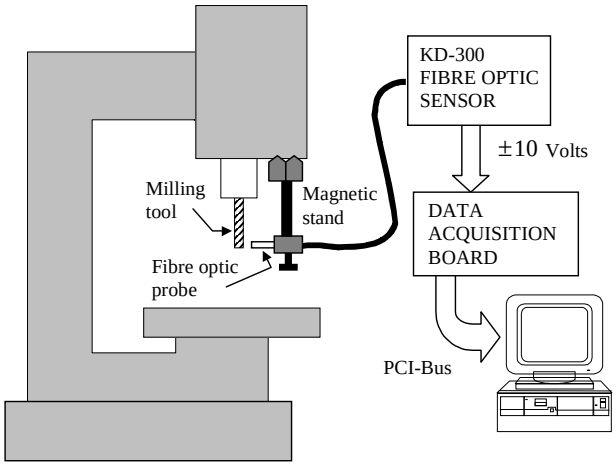

Fig.9. The experimental setup

3.1 Characterization of the sensor

The characterization of the sensor was made based on a specimen of a well-known geometry (cylindrical) which was made a groove, to determine the work range and the

characteristic equation The sensor was characterized using the equation (12).

$$y = \begin{bmatrix} 1.66 + 0.122x + .0029x^2 + 2.41*10^{-5}x^3 \\ -8.37*10^{-8}x^4 + 1.05*10^{-10}x^5 \end{bmatrix} \quad (12)$$

Obtained by polynomial regression with help of the compute tool (Equation Graper), that it is the distance of the sensor to the objective in function of the quantity of reflected light. In that way one has the characteristic equation of the reflection distance (fig. 10).

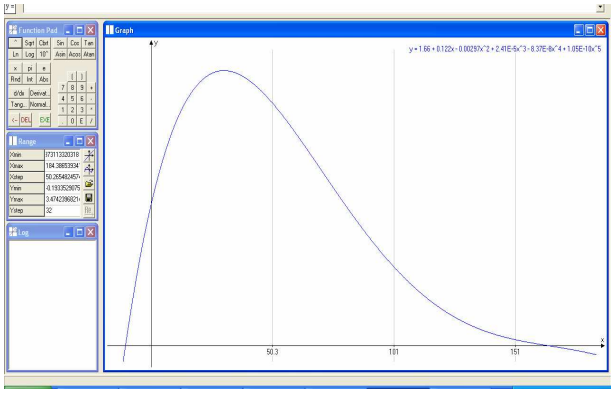

Fig 10 Response curve

The sensor was mounted in a magnetic base and was located in front of the rotating tool, as shown in Figure 11, with a gap of 2 mm to sense the tool profile during motion. The sensor is working on the front slope to increase the sensitivity of the measurement. The speed rotation of the main spindle was 300 RPM.

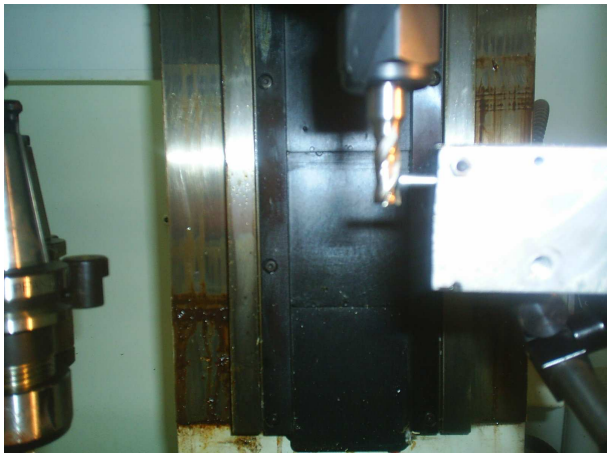

Fig. 11. Sensor and milling tool

4. RESULTS

The figure 12 shows the sensor response when one of the four flanks of the tool is worn. One can clearly identify the different flanks for each revolution of the tool. The circled area shows that the signal corresponding to the third flank varies respect to the other flanks due to wear. Figure 13 shows the corresponding polar plot of the output sensor using a new cutting tool. Since the sensor is located in front of the tool when it is rotating, the tool profile can be "reconstructed" after one tour. As it can be seen, the tool has four teeth with similar shape. Figure 14 shows the polar plot of the output sensor for a worn tool; the wear is located around 300 degrees of the tool profile, i.e., the third and fourth teeth are concerned.

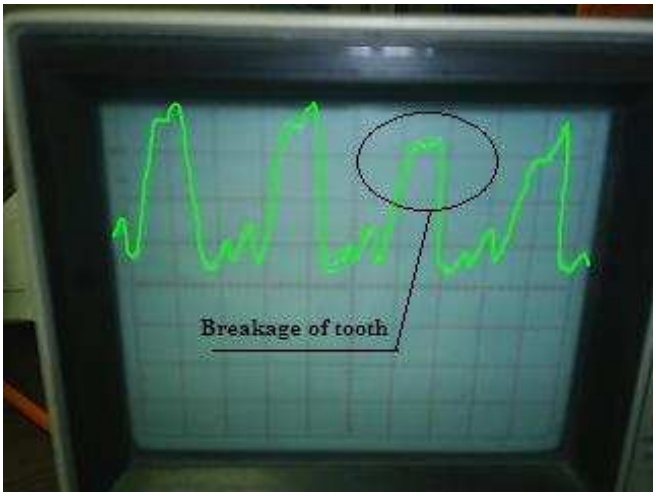

Fig 12. Sensor output plot while a worn tool is rotating

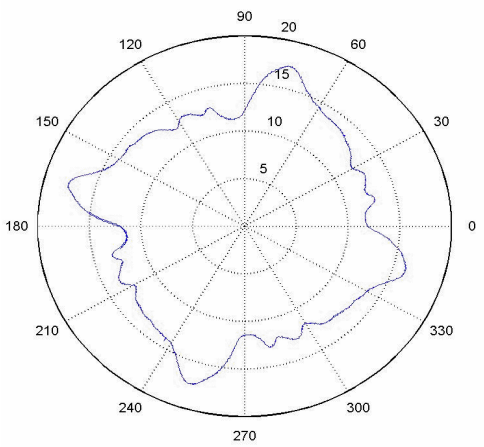

Fig. 13. Polar plots of new tool

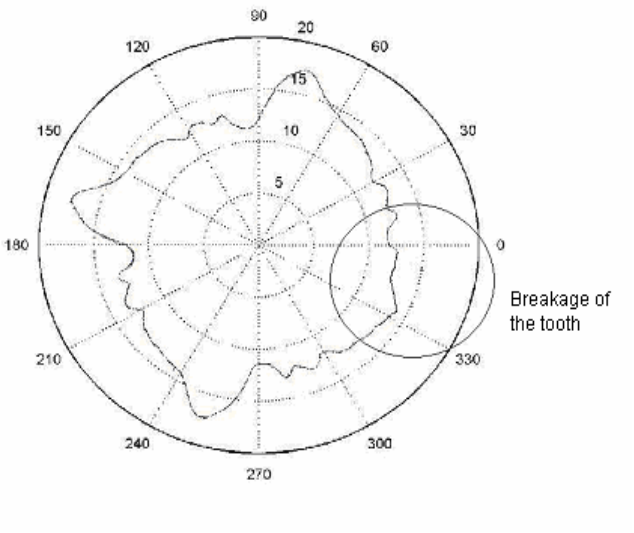

Fig. 14. Polar plots of worn tool

5. CONCLUSION AND FUTURE WORKS

A direct method for on-line wear detection of a rotating tool is presented. Instead of a high cost laser displacement sensor, this simple and low cost fiber optic sensor performs good quality measurements of the tool wear. The direct method developed has the ability to "reconstruct" the tool profile after only one tour of the tool, then it provides a very fast and accurate on-line method. In order to protect the sensor from sharp strips of metal, compressed air can be blown by a nozzle located near the sensor. The sensor response curve varies depending on the type of material of target surface, thus it has to be calibrated for each tool material. This technique can also be used in many other situations of on-line detection failures such as automatic crack detection of metal sheets**.**

AKNOWLEDGEMENTS

One of the authors (G. de A.) thanks to the Institute of Investigations in Optic Communications of the Autonomous University of San Luis Potosí (IICO-UASLP) ;as well as to San Luis Potosí's Technological Institute (ITSLP), also to the Department of Instrumentation and Control of the Autonomous University of Querétaro (UAQ), and to the Center of Engineering and Industrial Development (CIDESI), for the support that they offered him for the present investigation.

REFERENCES

[1]. Atam-4000 Control Station, "Operation Manual, Atam Systems Incorporated", Worthington, Ohio 43085, U.S.A., 1997.

[2]. Jemielniak, K. and Otman, O., "Catastrophic Tool Failure Detection Based on Acoustic Emission Signal Analysis", Annals of CIRP, Vol. 47/1, pp 31-34, 1998.

[3]. Meyer, W., Neumann, U., and Hörl, H., "Acoustic Emission Measurement for Quality Control and Process Monitoring in Cutting Operations", Report of the Technical University of Chemnitz, Faculty of Mechanical Engineering and Material Processing, Germany, 1996.

[4]. Kasashima, N., Mori, K., and Taniguchi, N., "On line Failure Detection in Face Milling Using Discrete Wavelet Transform", Annals of the CIRP, Vol. 44, pp. 483-487, 1995.

[5]. Barschdorff, D., Monostori, L., Kottenstede, T., Warnecke, G., and Müller, M., "Cutting Tool Monitoring in Turning under Varying Cutting Conditions: An Artificial Neural Network Approach", Proceedings of the Sixth International Conference on Industrial and Engineering Applications of Artificial Intelligence and Expert Systems, pp. 353-359, Edinburgh, Scotland, 1993.

[6]. Novak, A., "On–Line Prediction of the Tool Life", Annals of the CIRP, Vol. 45, pp. 93-96, 1996.

[7]. Kurada, S. and Bradley, C., "A review of machine vision sensors for tool condition monitoring", Computers and Industry, 34 (1), 1997, pp.55-72.

[8]. Oguamanam, D.C.D., Raafat, H., and Taboun, S.M., "A machine vision system for wear monitoring and breakage detection of single-point cutting tools", Computers in Industrial Engineering, 26 (3), 1994, pp. 245-251.

[9]. Wong, Y.S., Nee, A.Y.C., Li X.Q., Reisdorf, C., "Tool condition monitoring using a laser scatter pattern", Journal of Materials Processing Technology, Vol. 63, pp. 205-210, 1997.

[10]. Dimla, E. and Dimla, Snr., "Sensor signals for tool-wear monitoring in metal cutting operations-a review of methods", International Journal of Machine Tools & Manufacture", 40, 2000, pp. 1073-1098.

[11]. Ryabov, O., Mori, K., Kasashima, N., Uehara, K., "An In-process Direct Monitoring Method for Milling Tool Failures Using a Laser Sensor", CIRP Annals, Vol. 45, No.1, 1996.

[12]. Johnson, M., "Fiber Displacement Sensors for metrology and Control", Optical Engineering, Vol.24, No. 6, pp. 961-965, Nov./Dec., 1985.

[13]. Cook, R.O., and Hamm, C.W., "Fiber Optic Lever Displacement Transducer", Applied Optics, Vol. 18, pp. 3230-3240, Oct. 1, 1979.

[14]. Dakin, J., Culshaw, B., "Optical Fiber Sensors: Systems and Applications", Artech House Inc. 1989.

[15]. Larach, S., "Photo electronics Devices and Materials", Chapter 5, Van Nostrand, Princeton, N.J., 1965.

[16]. Hoogenboom, L., Allen, G.H., &Wang, S., "Theoretical and Experimental Analysis of a Fiber Optic Proximity Probe", S.P.I.E. Technical Symposium, East 84, Arlington, Virginia, April 29, 1984, Paper No. 478.